Targeted Imaging Agent to HSP70 Induced In Vivo

Pradip Ghosh, PhD[1] ⓘ, **Brian E. O'Neill, PhD[2]**, and **King C. Li, MD, FRCP, MBA[3]**

Abstract
Heat shock protein expression can be induced by heat shock making it possible to artificially modulate their levels noninvasively in vivo in a spatially and temporally controlled manner. Here, we report the use of the major heat shock protein 70 (HSP70) as an inducible target by using the small molecule deoxyspergualin (DSG) conjugated to the near-infrared fluorophore (Cy5.5). We demonstrate that heat induction in the form of localized hyperthermia of normal tissue in living mice results in sufficient HSP70 overexpression for detection with DSG-Cy5.5 conjugate. This effect is dependent on total energy delivered and reaches maximum fluorescence signal in 6 to 8 hours post heat induction and declines over a period of up to 24 hours. These results suggest that DSG-Cy5.5 agent accumulates in tissue with elevated HSP70 by heat.

Keywords
heat shock proteins, HSP70, deoxyspergualin, Cy5.5, near-infrared fluorescence, DSG

Introduction

Heat shock protein 70 (HSP70), is a molecular chaperone, has strong cytoprotective effects and can help in maintaining the proper conformation of other proteins after a large variety of stresses.[1-6] Stress can be any sudden change in environment such as heat shock, oxidative stress, heavy metals, or anticancer drugs. Stress causes increased amount of damaged proteins by inhibiting their elimination via the proteasome as well as by damaging the chaperones themselves. Heat shock proteins (HSPs) are generally classified according to their molecular weights with the majority belonging to the groups HSP27, HSP40, HSP60, HSP70, HSP90, and large HSPs (HSP110 and glucose-regulated protein 170).[7] Except for the group of small HSPs, HSP proteins are adenosine triphosphate (ATP)-dependent proteins with ATPase activity.[5] Heat shock protein 70 family members possess a C-terminus domain that chaperones unfolded proteins and peptides, and an N-terminus ATPase domain that controls the opening and closing of the peptide-binding domain.[3] It can form stable complexes with cytoplasmic tumor antigens that can then escape intact from dying cells. Heat shock protein 70 proteins have crucial functions in protein folding, the maintenance of protein homeostasis, and enhancement of cell survival following a multitude of stresses.[8] Heat shock proteins are implicated in tumor cell proliferation, differentiation, invasion, metastasis, death, and recognition by the immune system.

Several group reported the roles of HSP70s in cancer.[9-11] Heat shock protein 70s play important roles in cancer development and are often expressed at abnormally high levels in cancer cells. Heat shock protein 70s promote carcinogenesis by acting as survival factors owing to their tumor-associated expression and antiapoptotic effects.[12] Jäättelä et al reported that HSP70 protected cancer cells from TNF-induced cytotoxicity, and they suggested that HSP70 may increase the oncogenic potential of some cancer cells via an immunological escape mechanism.[13] The roles of HSP70s in cancer development may be a potential theranostic target for cancer therapy.[14-18]

High HSP70 levels are associated with adverse outcomes in breast, endometrial, oral, colorectal, prostate cancers, and certain leukemias.[5,19-21] Moreover, transgenic overexpression of Hsp70 is sufficient to induce T-cell lymphoma in some

[1] Department of Neurology, UT Medical School, University of Texas Health Science Center, Houston, TX, USA
[2] Department of Radiology, The Methodist Hospital Research Institute, Houston, TX, USA
[3] Carle Illinois College of Medicine, University of Illinois, Champaign, IL, USA

Corresponding Author:
Pradip Ghosh, Department of Neurology, UT Medical School, University of Texas Health Science Center, 6565 Fannin Street, Houston, TX 77030, USA.
Email: pghosh38@yahoo.com

models.[20] This observation is important because induction of HSP70 can be misregulated in cancer, potentially mediated by altered activity of the heat shock transcription factor 1.[22-24] Despite the role of HSPs in cancer biology, the precise mechanism remains largely unknown yet.

In an effort to elucidate the role of heat shock proteins, we set out to generate a new probe selective for the classically defined heat-inducible protein (HSP70). Among the potential chemical ligands specific for HSP70, we have selected a derivative of spergualin, 15-deoxyspergualin (DSG) a potent immunosuppressive agent with antitumor properties,[25-31] which was also found to biochemically bind to HSP70 and HSP90.[25,32] Although the precise mechanism of action of DSG remains unknown, the antitumor effect of DSG is thought to be mediated by inhibition of cell cycle progression at G1 phase or by affecting angiogenesis.[33-35] Nonetheless, these pleiotropic effects may also be explained by mechanisms that involve modulation of heat shock proteins. Deoxyspergualin was originally developed in Japan as an immunosuppressive agent but this compound is not commercially available. Several groups synthesized this compound but they reported low yields (7%-12%).[36-46]

In this report, we describe an improved DSG synthesis according to the published methods with some major modification of reaction conditions with high yields (overall 18%-22%). Recently, several groups developed and evaluated the HSP-targeted imaging agents.[47-50]

Using this HSP70-selective ligand, we set out to test our hypothesis for enhancing the intracellular targeting of an inducible protein on demand. We conjugated a fluorophore to the selective ligand (DSG) for in vitro cellular uptake and in vivo imaging studies. We found that this compound accumulates within heat shocked cells and muscle tissue treated with locoregional hyperthermia in mice. We believe these findings have significant implications for developing new HSP-targeted optical imaging agents.

Materials and Methods

Reagents and Instrumentations

All reagents and solvents were purchased from Aldrich Chemical Co and used without further purification. Thin-layer chromatography (TLC) was performed on precoated Kieselgel 60 F254 (Merck) glass plates. Proton and Carbon NMR spectra were recorded on a Brucker 300 or 500 MHz spectrometer using tetramethylsilane as an internal reference and hexafluorobenzene as an external reference, respectively, at The University of Texas MD Anderson Cancer Center. The mass spectra were obtained on a LCQ Fleet mass spectrometer using electrospray ionization technique. Microwave synthesis was performed on a Biotage Initiator Eight microwave synthesizer. High-performance liquid chromatography (HPLC) was performed on a 1200 series pump (Agilent), with UV detector operated at 254 or 690 nm, using a semipreparative and analytical C-18 reverse phase column, Luna SCX 100A (5 μm, 250

× 10 mm) or Vydac protein and peptide C-18 column (5 μm, 150 × 4.6 mm).

Chemistry

7-Bromoheptanamide: 1. 7-bromoheptanenitrile (3.0 g, 15.78 mmol) was dissolved in 50 mL of concentrated hydrochloric acid and stirred for 8 hours at 40 °C. The mixture was then poured onto ice-cold water (200 mL). The white precipitate was obtained and filtered off. Washed with water and evaporated to dryness. The crude product is crystallized from ethyl acetate-methylcyclohexane solvent mixture to give 2.67 g of the expected product **1** in the form of white crystals (81% yields). ^{1}H NMR **1** (CDCl$_3$) δ: 1.33-1.53 (m, 4H), 1.65 (m, 2H), 1.88 (m, 2H), 2.24 (t, $J = 6.0$, 2H), 3.40 (t, J = 6.0, 2H), 5.41 (m, 1H), 5.7 (m, 1H). MS: M + 1, calculated 209.09, found 209.12.

7-Azidoheptanamide: 2. To a solution of compound **1** (2.5 g, 12.01 mmol) in dimethyl sulfoxide (15 mL) was added sodium azide (1.56 g, 24.03 mmol). The mixture was heated by microwaves synthesizer in a sealed tube at 100 °C for 2 hours. The mixture was dissolved in ethyl acetate (150 mL) and washed with water (3 × 150 mL). The organic phase was dried (MgSO$_4$), evaporated to dryness and purified on a silica gel column and using 5% isopropanol in ethyl acetate as eluent. This afforded product **2** as a white solid (1.5 g, 74% yield). ^{1}H NMR **2** (CDCl$_3$) δ: 1.38-1.41 (m, 4H), 1.56-1.74 (m, 4H), 2.25 (t, $J = 7.4$, 2H), 3.27 (t, $J = 9.0$, 2H), 5.72 (m, 2H). MS: M + 1, calculated 171.213, found 171.218.

Acetic Acid, [(7-Azido-oxoheptyl)amino]hydroxymethyl ester: 3. Compound **2** (1.0 g, 5.88 mmol) and 1 g of 4Å molecular sieves was dissolved in dichloromethane (30 mL) in a flask under argon filled balloon. 2-hydroxy-2-methoxy acetate (0.70 mL, 7.05 mmol) was added to the mixture and refluxed for 12 hours. Molecular sieves were removed by filtration and solvent was evaporated to dryness under vacuum. The crude residue was dissolved in dichloromethane (60 mL) and washed with water (3 × 60 mL). The organic phase was dried (MgSO$_4$), evaporated to dryness and purified by flash chromatography using 2% methanol in dichloromethane. The pure compound **3** (1.2 g) was obtained as a solid in 70% yield. ^{1}H NMR **3** (CDCl$_3$) δ: 1.35-1.40 (m, 4H), 1.55-1.63 (m, 4H), 2.27 (t, $J = 7.1$, 2H), 3.26 (t, $J = 6.3$, 2H), 3.86 (s, 3H), 4.27 (d, $J = 6.0$, 1H), 5.60 (dd, $J = 6.1$, $J = 7.0$, 1H), 6.72 (d, $J = 7.0$, 1H). MS: M + 1, calculated 259.227, found 259.232.

Acetic acid, [(7-azido-oxoheptyl)amino][1-(2-naphthalenyl) ethoxy], methyl ester: 4. Compound **3** (1.0 g, 3.87 mmol) was dissolved in dichloromethane (20 mL) in a dry flask under argon atmosphere and thionyl chloride (0.4 mL, 5.42 mmol) was added dropwise into the mixture. The resulting mixture was refluxed at 50 °C for 1 hour, cooled and concentrated under reduced pressure. After that, the crude chloroglycine derivative was dissolved in 15 mL of dichloromethane and then (S)-(-)-α-methyl-2-naphthalenemethanol (0.73 g, 4.26 mmol) in 5 mL

of dichloromethane was added dropwise followed by addition of triethylamine (1.08 mL, 7.74 mmol). The reaction mixture was stirred at room temperature for 12 hours when TLC showed that no significant starting material remained. The crude mixture was dissolved in dichloromethane (85 mL) and washed with 1(N)HCl (100 mL) and then brine (100 mL). The organic layer was dried (MgSO$_4$), concentrated and crude residue was purified by a silica gel column using 1% isopropanol in hexane as eluent to give 1.2 g (75%) of a mixture of diastereomeric esters, which was directly used in the next step. ^{1}H NMR **4** (CDCl$_3$) δ: 1.34-1.40 (m, 4H), 1.48 (d, J = 6.3, 3H), 1.54-1.74 (m, 4H), 2.20-2.42 (m, 2H), 3.28 (t, J = 6.6, 2H), 3.80 (s, 3H), 4.97 (q, 1H), 5.55 (d, J = 9.3, 1H), 6.54 (d, J = 9.2, 1H), 7.42-7.54 (m, 3H), 7.80-7.88 (m, 4H). MS: M + 1, calculated 432.524, found 432.529.

2-[(7-Azido-1-oxoheptyl)amino]-2-[1-(S)-(naphthalen-2-yl)ethoxy]acetic acid: 5.

Compound **4** (2.8 g, 6.8 mmol) was taken in a round bottom flask and dissolved in 1,2-dimethoxyethane (40 mL). 1(N) sodium hydroxide (8.2 mL, 8.15 mmol) solution was added to the mixture and stirred for 1 hour at room temperature. The solvent was evaporated, residue was diluted with water (100 mL) and acidified with 1(N) hydrochloric acid (pH 2-3). The aqueous phase was extracted with ethyl acetate (3 × 100) and the organic phase was dried (MgSO$_4$) and concentrated under reduced pressure to yield 2.6 g (96%) of the crude diastereomeric mixture of acids **5** in the form of oil. ^{1}H NMR **5** (CDCl$_3$) δ: 1.26-1.33 (m, 8H), 1.53 (d, J = 7.1, 3H), 1.68 (bs, 2H), 2.06-2.16 (m, 2H), 4.34 (t, J = 7.2, 1H), 5.64 (d, J = 8.2, 1H), 7.43-7.49 (m, 1H), 7.68-7.75 (m, 3H), 7.84-8.0 (m, 4H), 12.23 (bs, 1H). MS: M + 1, calculated 399.454, found 399.462.

N^4-Tert-Butoxycarbonyl-1,4-Butanediamine: 6.

1, 4 diaminobutane (4.0 g, 45.38 mmol) was dissolved in tetrahydrofuran (50 mL) under argon, triethylamine (12.76 mL, 90.76 mmol) was added, followed by addition of 4-dimethylamino pyridine (1.7 g, 13.61 mmol). The mixture was cooled to 0 °C then di-tert-butyl dicarbonate (11.89 g, 54.45 mmol) was added via a syringe over a period of 30 minutes. The reaction mixture was warmed to room temperature and stirred for 6 hours when TLC showed that no starting material remained. The solvent was evaporated under vacuum; the residue was dissolved in dichloromethane (150 mL) and washed with water (3 × 150 mL). The organic phase was dried (MgSO$_4$), evaporated to dryness and purified on a silica gel column using 2% methanol in dichloromethane as eluent. The pure compound **6**, 5.8 g was obtained in 68% yield. ^{1}H NMR **6** (CDCl$_3$) δ: 1.25 (s, 9H), 1.55 (t, J = 7.2, 2H), 2.02 (bs, 2H), 2.21 (bs, 2H), 2.84 (t, J = 6.6, 2H), 3.63 (t, J = 6.1, 2H), 7.11 (bs, 1H). MS: M + 1, calculated 189.266, found 189.269.

N^4-tert-butoxycarbonyl-N^1-(2-cyanoethyl)-1,4-butanediamine: 7.

A solution of compound 6 (3.0 g, 15.93 mmol) in dry methanol (10 mL) was cooled to −10 °C for 10 minutes under argon. Acrylonitrile (1.01 g, 19.12 mmol) was slowly added via a syringe over a period of 5 minutes. The reaction mixture was stirred at −10 °C for 1 hour, warmed to room temperature and continued for overnight when TLC showed that no starting material remained. Solvent was evaporated under vacuum. The residue was purified on a silica gel column using 2% methanol in dichloromethane as eluent. The pure compound 7, 2.8 g was obtained in 74% yield. ^{1}H NMR 7 (CDCl$_3$) δ: 1.40 (bs, 9H), 1.46-1.50 (m, 4H), 1.60 (s, 1H), 2.49 (t, J = 6.6, 2H), 2.62 (t, J = 6.6, 2H), 2.88 (t, J = 6.6, 2H), 3.03 (t, J = 7.1, 2H), 7.01 (bs, 1H). MS: M + 1, calculated 242.320, found 242.328.

N^1-Benzyloxycarbonyl-N^4-tert-butoxycarbonyl-N^1-(2-cyanoethyl)-1,4-butanediamine: 8.

Compound **7** (4.2 g, 17.40 mmol) and triethylamine (5 mL, 34.81 mmol) was dissolved in tetrahydrofuran (40 mL) under argon. The mixture was cooled to 0 °C and then benzyl chloroformate (3.0 g, 17.44 mmol) in tetrahydrofuran (10 mL) was added dropwise over a period of 1 hour. The reaction mixture was warmed to room temperature and stirred for 4 hour when TLC showed that no starting material remained. A precipitate was removed by filtration and filtrate was evaporated to dryness under vacuum. The residue was purified on a silica gel column using 20% methanol in dichloromethane as eluent. The pure compound **8**, 4.1 g was obtained in 76% yield. ^{1}H NMR **8** (CDCl$_3$) δ: 1.43 (d, J = 4.5, 10H), 1.54 (bs, 3H), 2.60 (dd, 2H), 3.11 (bs, 2H), 3.36 (t, J = 6.6, 2H), 3.52 (t, J = 6.5, 2H), 5.14 (s, 2H), 7.21 (bs, 1H), 7.30-7.42 (m, 5H). MS: M + 1 calculated 376.466, found 376.471.

N^4-Benzyloxycarbonyl-N^8-tert-butoxycarbonylspermidine: 9.

A solution of compound **8** (3.0 g, 7.99 mmol) in dry ethyl ether (50 mL) was cooled to 0 °C for 10 to 15 minutes under argon atmosphere. A suspension of lithium aluminium hydride (1.06 g, 27.97 mmol) in dry ethyl ether (50 mL) was added dropwise to this mixture. The reaction mixture was stirred at 0 °C for 1 hour and quenched by the addition of water (1 mL) and ethyl acetate (10 mL). The resulting suspension was filtered through a celite pad and washed with ethyl acetate (3 × 30 mL). The solvent was evaporated and treated with 1(N) HCl in dioxane (3 mL). The solvent was evaporated, residue was dissolved in water (100 mL), and extracted with ethyl acetate (3 × 100 mL). The organic layer was discarded and the aqueous layer was alkalized to pH 8 to 9 (saturated sodium bicarbonate solution) and extracted with chloroform (3 × 100 mL). The organic layer was evaporated, dried over MgSO$_4$ and purified on a silica gel column using 5% methanol in dichloromethane to isolate **9** (1.9 g) in 63% yield as yellow oil. ^{1}H NMR **9** (CDCl$_3$) δ: 1.36-1.45 (m, 9H), 1.46-1.55 (m, 4H), 1.64 (t, J = 6.9, 2H), 2.16 (s, 2H), 2.76 (t, J = 6.3, 2H), 3.01-3.18 (m, 6H), 4.64 (bs, 2H), 6.98 (bs, 1H), 7.30-7.42 (m, 5H). MS: M + 1 calculated 380.492, found 380.498.

N^1, N^4-Dibenzyloxycarbonyl-N^8-tert-butoxycarbonylspermidine: 10.

Compound **9** (2.0 g, 5.27 mmol) and triethylamine (1.5 mL, 10.54 mmol) was dissolved in tetrahydrofuran (30 mL) under argon atmosphere. The mixture was cooled to 0 °C and then benzyl chloroformate (0.99 g, 5.80 mmol) in tetrahydrofuran (10 mL) was added dropwise over a period of 1 hour. The reaction mixture was warmed to room temperature and stirred

for 4 hours when TLC showed that no starting material remained. A precipitate was removed by filtration and filtrate was evaporated to dryness under vacuum. The residue was dissolved in ethyl acetate (100 mL) and washed with water (3 × 100 mL). The organic phase was dried (MgSO$_4$), evaporated to dryness, and purified on a silica gel column using 2% Methanol in dichloromethane afforded **10** (1.9 g, 70%) as an oil. ^{1}H NMR **10** (CDCl$_3$) δ: 1.36-1.45 (bs, 11H), 1.46-1.52 (bs, 2H), 1.71 (t, J = 6.0, 2H), 3.0-3.22 (m, 4H), 3.23-3.34 (m, 4H), 5.12 (bs, 4H), 7.01(br, 2H), 7.35-7.40 (m, 10H). MS: M + 1 calculated 514.622, found 514.626.

N^1, N^4-bis (benzyloxycarbonyl) spermidine: 11. Compound **10** (2.0 g, 3.9 mmol) was dissolved in dichloromethane (30 mL) under argon atmosphere. Trifluoroacetic acid (6 mL, 78.0 mmol) was added dropwise to the mixture and stirred for 30 minutes at 0 °C and 3 hours at room temperature when TLC showed no starting material remained. Solvent was evaporated and crude residue was purified on a silica gel column using 5% methanol in dichloromethane to isolate **11** (1.3 g) in 81% yield. ^{1}H NMR **11** (CDCl$_3$) δ: 1.66 (bs, 4H), 1.67-1.80 (m, 2H), 2.94 (bs, 2H), 3.11 (bs, 2H), 3.15-3.35 (m, 4H), 5.02 (bs, 4H), 5.93 (bs, 2H), 7.27-7.36 (m, 10H), 7.88 (bs, 1H). MS: M + 1 calculated 414.537, found 414.542.

Tetraazaheneicosanoic acid, azido[1-(2-naphthalenyl)ethoxy] dioxo[(phenylmethoxy)carbonyl] phenylmethyl ester: 12. Compound **5** (2.5 g, 6.27 mmol) was dissolved in dichloromethane (60 mL) in a dry flask under argon and hydroxybenzotriazole (0.85 g, 6.27 mmol) was added followed by addition of N, N′dicyclohexylcarbodiimide (1.42 g, 6.9 mmol). The reaction mixture stirred for 2 hours at room temperature and N^1, N^4-bis(benzyloxycarbonyl)spermidine, Compound **11** (2.85 g, 6.9 mmol) was added. The reaction mixture was further stirred for 12 hours at room temperature when TLC showed no starting material remained. Solvent was evaporated under vacuum and the residue was dissolved in dichloromethane (100 mL) and washed with saturated aqueous sodium bicarbonate (3 × 100 mL). The organic phase was dried (MgSO$_4$), evaporated to dryness and the crude product was purified on a silica gel column using 3% isopropanol in ethyl acetate as eluent to give 4.1 g (82%) of a mixture of epimers which was directly used in the next step. ^{1}H NMR **12** (DMSO-d_6) δ: 1.22-1.53 (m, 17H), 2.10-2.41 (m, 2H), 2.91-3.18 (m, 8H), 3.42 (t, J = 6.3, 2H), 4.80 (q, J = 6.0, 1H), 5.10 (s, 2H), 5.12 (s, 2H), 5.18 (d, J = 9.1, 1H), 7.11-7.39 (m, 11H), 7.43-7.56 (m, 3H), 7.82 (s, 1H), 7.83-8.13 (m, 3H), 8.16-8.20 (m, 1H), 8.65 (d, J = 9.0, 1H). MS: M + 1, calculated 794.952, found 794.957.

Hexa-azapentacos-2-enedioic acid, 13-[1-(2-naphthalenyl) ethoxy]dioxo[(phenylmethoxy)-carbonyl]-3-[[(phenylmethoxy) carbonyl]amino]bis(phenylmethyl) ester: 13a and *Hexa-azapentacos-2-enedioic acid, 13-[1-(2-naphthalenyl)ethoxy]dioxo[(phenylmethoxy)-carbonyl]-3-[[(phenylmethoxy)carbonyl]amino]bis(phenylmethyl) ester: 13b*. Compound **12** (3.6 g, 4.53 mmol) and triphenylphosphine (1.19 g, 4.53 mmol) were dissolved in tetrahydrofuran

(15 mL) and water (3 mL) at the ratio of 5:1. The reaction mixture was then heated by microwaves synthesizer in a sealed tube at 80 °C for 4 hours. Cooled the reaction mixture and N, N-bis(benzyloxycarbonyl)-S-methylisothiourea (1.79 g, 5.0 mmol) was added and stirred for 2 hours at room temperature when TLC showed no significant starting material remained. Concentrated the mixture of epimers, which was purified and separated by flash chromatography using 3% isopropanol in ethyl acetate to produce **13a** (2.0 g, 41%) and **13b** (1.8 g, 37%) as an oil. ^{1}H NMR **13a** (CD$_3$CN) δ: 1.31-1.60 (m, 14H), 1.49 (d, J = 7.3, 3H), 2.17 (t, J = 7.1, 2H), 2.94-3.0 (m, 2H), 3.10-3.21 (m, 6H), 3.34 (m, 2H), 4.88 (q, J = 6.0, 1H), 5.05-5.16 (4s, 8H), 5.24 (d, J = 9.0, 1H), 5.72-5.94 (2m, 1H), 6.90-7.41 (m, 22H), 7.42-7.53 (m, 3H), 7.80-8.0 (m, 4H), 8.27 (br, 1H), 11.81 (s, 1H). MS: M + 1, calculated 1079.256, found 1079.262. ^{1}H NMR **13b** (CD$_3$CN) δ: 1.27-1.58 (m,14H), 1.48 (d, J = 7.5, 3H), 2.18 (t, J = 7.1, 2H), 2.94-3.06 (m, 2H), 3.08-3.22 (m, 6H), 3.34 (m, 2H), 4.88 (q, J = 6.0, 1H), 5.01-5.18 (4s, 8H), 5.22 (d, J = 9.1, 1H), 5.70-5.89 (2m, 1H), 6.95-7.41 (m, 22H), 7.44-7.56 (m, 3H), 7.82-8.12 (m, 4H), 8.30 (br, 1H), 11.82 (s, 1H). MS: M + 1, calculated 1079.254, found 1079.257.

7-[(Aminoiminomethyl)amino]-N-[2-[[4-[(3-aminopropyl)amino] butyl]amino]-1-hydroxy-2-oxoethyl]heptanamide-tris hydrochloride: (DSG), 14. Compound **13a** (1.0 g, 0.93 mmol) was dissolved in 1(N) acetic acid in methanol (100 mL) under nitrogen atmosphere. To this solution, 0.3 g (50 wt%) of palladium hydroxide (Pearlman's catalyst, 20% on carbon/50% water) was added and stirred for overnight under 1 atm of hydrogen at room temperature. The mixture was filtered. In the filtrate, 0.3 g (50 wt%) of Pearlman's catalyst was added again and further stirred for 4 hours at room temperature. The reaction mixture was filtered and concentrated under reduced pressure. The residue was dissolved in water (50 mL) and washed with dichloromethane (3 × 50 mL). The aqueous phase was lyophilized. The tris-acetate form of the compound was transformed into its tris-hydrochloride form by the following procedure. The powder was dissolved in H$_2$O (20 mL) and the pH of the solution was adjusted to 2 to 3 by a slow addition of 1(N)HCl at 0 °C and the solution was lyophilized. The resulting powder was dissolved in water (20 mL) and lyophilized again to give the tris hydrochloride **14** as a hygroscopic white powder (0.27 g, 75%). The chemical purity was determined by an analytical HPLC using a C-18 Vydac protein and peptide column (5 μm, 150 × 4.6 mm). The mobile phase starting from 95% solvent A (0.1% trifluoroacetic acid in water) and 5% solvent B (0.1% trifluoroacetic acid in acetonitrile; 0-3 minutes) to 20% solvent A and 80% solvent B for 25 minutes. Flow rate was 1 mL/min, temperature 31 °C. ^{1}H NMR **14** (D$_2$O) δ: 1.30 (m, 4H). 1.55 (m, 8H), 2.06 (m, 2H), 2.22 (t, J = 7.5, 2H), 3.10 (m, 6H), 3.24 (m, 4H), 5.35 (s, 1H). ^{13}C NMR **14** (D$_2$O) δ: 22.3, 25.3, 25.7, 26.4, 26.6, 28.4, 29.0, 36.1, 37.4, 40.0, 42.3, 45.4, 48.2, 71.9, 156.8, 171.4, and 178.2. MS: HRMS (M + 1): calculated 388.2508, found 388.2511.
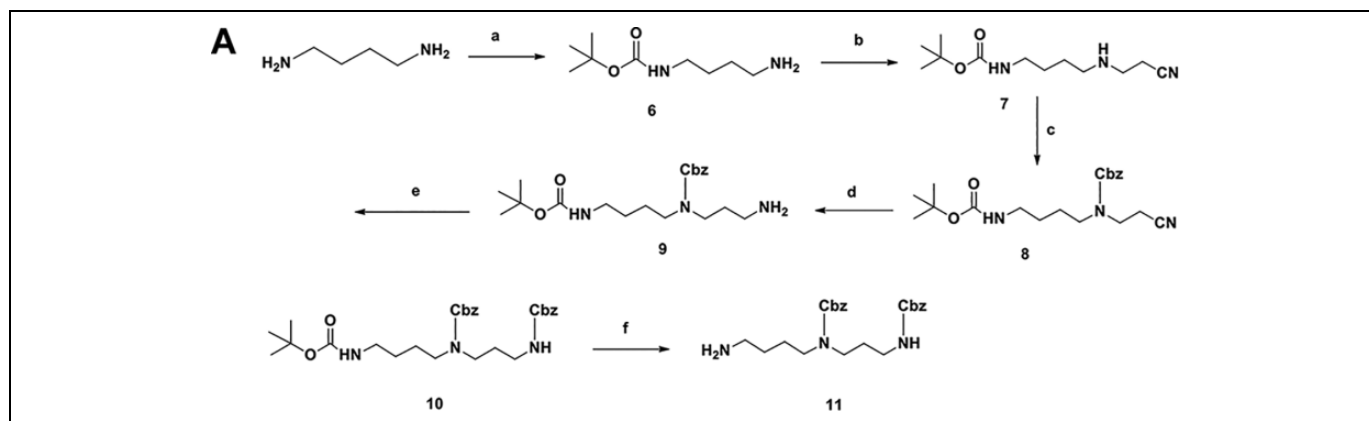
Figure 1(A). A, Synthetic scheme of protected spermidine. ***Reagents and reaction conditions:*** (a) t-BOC, THF, Et$_3$N, DMAP, rt, 6h, 68%; (b) Acrylonitrile, MeOH, -10°C, rt, overnight, 74%; (c) Cbz-Cl, Et$_3$N, THF, rt, 4h, 76%; (d) LAlH4, Et$_2$O, 0°C, 1(N) HCl, 63%; (e) Cbz-Cl, Et$_3$N, THF, rt, 4h, 70%; (f) TFA, DCM, rt, 3h, 81%.
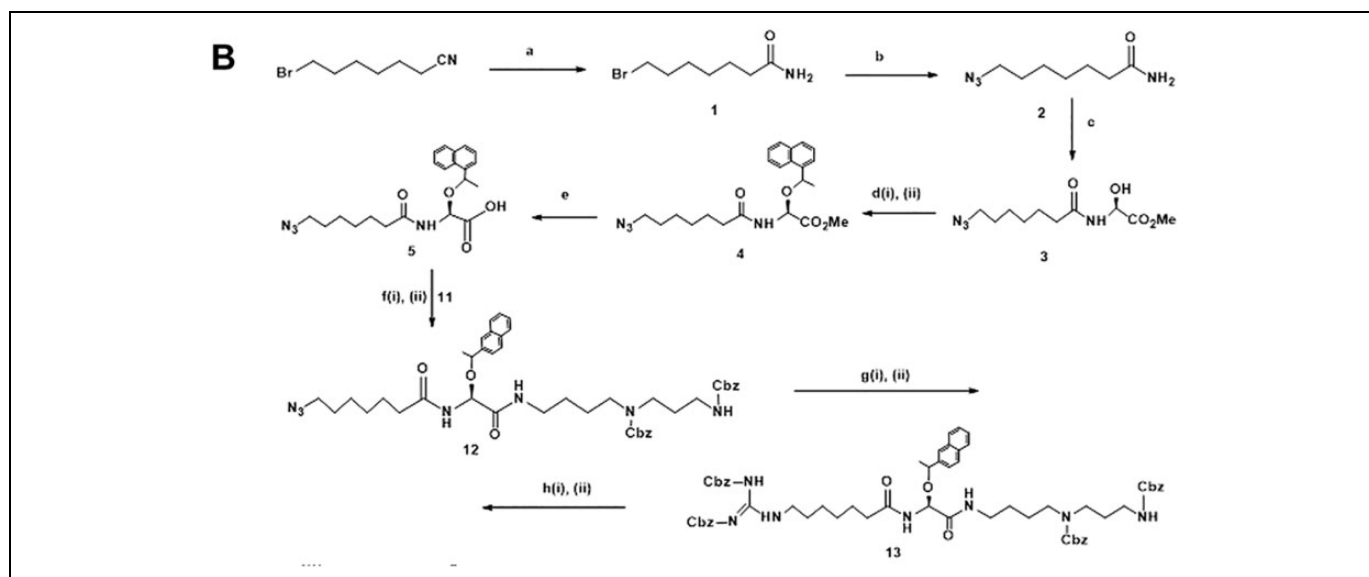

Figure 1(B). Synthetic scheme of deoxyspergualin (DSG) ***Reagents and reaction conditions:*** (a) HCl, 40°C, 8h, 81%; (b) NaN$_3$, DMSO, 100°C, 2 h, microwave, 74%; (c) (MeO)(HO)CHCO$_2$Me, DCM, 40°C, 12 h, molecular sieves 4 Å, 70%; d(i) SOCl$_2$, DCM, 50°C, 1 h; d(ii) (S)-2-NaphtCH(OH)Me, DCM, Et$_3$N, rt, 12 h, 75%; (e) 1(N)NaOH, DME, rt, 1h, 96%; f(i) DCC, HOBt, DCM, rt, 2h, f(ii) H$_2$N(CH$_2$)$_4$N(Cbz)(CH$_2$)$_3$NHCbz, rt, 12, 82%; g(i) Ph$_3$P, H$_2$O, THF, 80°C, 4h, microwave; g(ii) CbzN=C(SMe)NHCbz, THF, rt, 3h, Flash chromatography, 78% (total); h(i) Pd(OH)$_2$/C, MeOH/AcOH, H$_2$, 1 atm, h(ii) 1(N)HCl, pH 2-3, HPLC, 75%.

DSG-Cy5.5 conjugates: 15. Compound **14**, DSG (2 mg, 0.005 mmol) was dissolved in 0.3 mL of 0.1M sodium phosphate buffer (pH 8.2) and mixed with Cy5.5 mono NHS ester (8.7 mg, 0.007 mmol) in DMSO (50 µL). The reaction mixture was stirred in the dark at ambient temperature overnight and then quenched by adding 50 µL of 5% acetic acid in water. The crude product was purified by a semipreparative C-18 Vydac protein and peptide column (5 µm, 250 × 10 mm). The flow was 1 mL/min, with the mobile phase starting from 90% solvent A (0.1% trifluoroacetic acid in water) and 10% solvent B (0.1% trifluoroacetic acid in acetonitrile) to 10% solvent A and 90% solvent B for 20 minutes. The fraction containing desired

conjugate DSG-Cy5.5 was collected, evaporated, and stored in the dark at −20 °C until use. The pure conjugate **15**, 4.0 mg was obtained in 60% yield. The purified DSG-Cy5.5 conjugate was characterized by high resolution mass spectroscopy (HRMS). HRMS (M + 1): calculated 1303.4550, found 1303.4555.

In Vitro Cellular Uptake Studies

Immunohistochemical staining procedure. Human lung carcinoma cells (A549) were plated at a density of approximately 10 000 per chamber in a 96-well clear bottom black plate using Dulbecco's Modified Eagle Media (DMEM) supplemented with
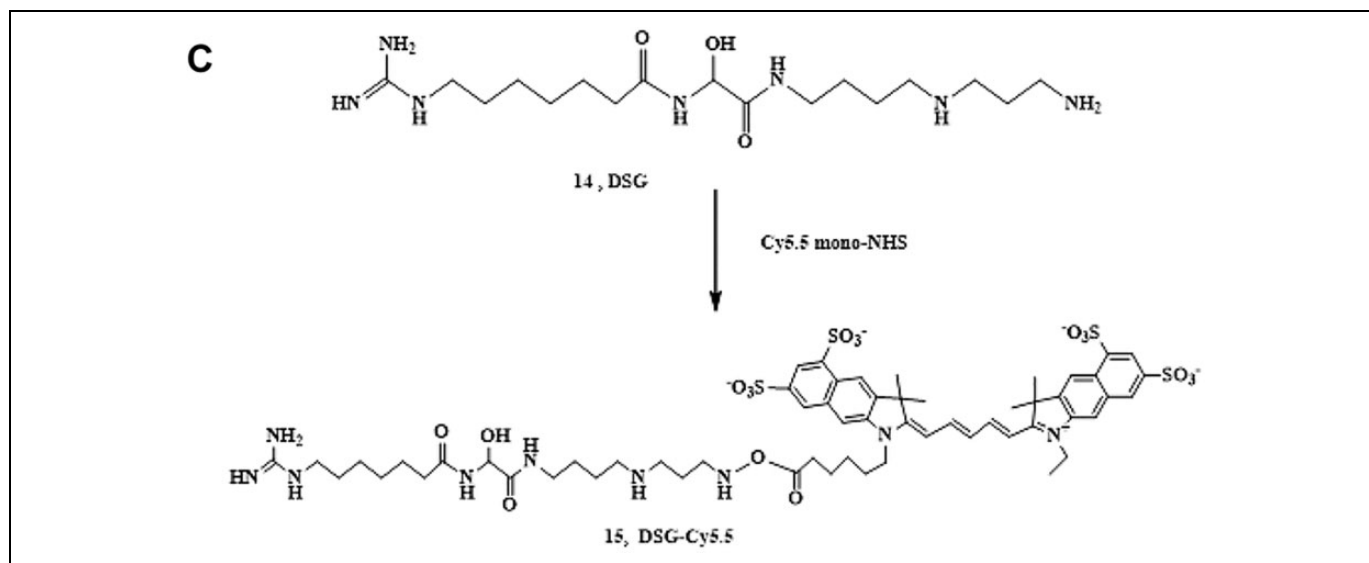
Figure 1(C). C, Synthetic scheme of DSGCy5.5. ***Reagents and reaction conditions:*** $Na_2B_4O_7$, rt, overnight, HOAc, HPLC, 60%.

10% fetal bovine serum (FBS), 50 U/mL of penicillin and 50 µg/mL streptomycin, and grown overnight at 37 °C. Fixing was achieved with 4% formaldehyde in phosphate-buffered saline (PBS) for 30 minutes and the subsequent staining procedure was performed as described in the antibody supplier's instruction manual (R&D Systems, Inc). As an additional positive control, A549 cells were treated with 1 mM $CuSO_4$ for 24 hours as described by Neuhaus-Steinmetz and Rensing[51] followed by fixing and anti-HSP70 antibody staining. Primary antibody detection was performed with a fluorescein-labeled secondary antibody as described by the supplier. Nucleic acid counterstaining with DAPI (4′,6-diamidino-2-phenylindole) was achieved immediately after acquisition of fluorescence microscopy images (Figure 2) while on the microscope stage and then photographed with the appropriate filter.

Cultured cells heat shock procedure. A549 human lung carcinoma cells were grown in a 24-well plate at a density of 400 000 cell/well using DMEM supplemented with 10% FBS and 50 U/mL of penicillin and 50 µg/mL streptomycin in a total of 2 mL. They were allowed to attach for 24 hours prior to heat shock. Cells were heated at 41 °C to 42 °C for 1 hour or 43 °C for 10 minutes (Figure 3) in a humidified incubator with 5% CO_2 followed by immediate recovery at 37 °C. During the heat shock period, the temperature was monitored with the use of a micro-thermocouple inserted into a 96-well plate chamber containing the same volume of culture media. Following recovery for approximately 6 hours, DSG-Cy5.5 conjugate was directly added to the culture media at a 3 different concentration of 1, 5, and 10 µM; and incubated for 1 hour at 37 °C. Cells were then washed 3 times with prewarmed PBS (37 °C), followed by scrap harvesting, counted, and diluted to 100 000 cells/mL. Approximately 10 000 cells per well were seeded in 96-well black plates and measured in a fluorometric plate reader (FLUOstar OPTIMA) with a 620/700 nm filter at an

optical magnification of ×20. As an additional control, cells treated with $CuSO_4$ were also tested for uptake of DSG-Cy5.5 (Figure 4). Phase-contrast images were obtained with each view.

In Vivo Hyperthermia Imaging

Approximately 6-week-old bagg albino mice (BALB/c) nu/nu female mice were purchased from Charles River Laboratories and maintained on a regular diet. A heating apparatus was constructed to permit localized deposition of heated water to one (right hind) limb of each mouse (Figure 5). For anesthesia, mice were induced with 4% isoflurane and maintained on 2% throughout the entire heating procedure. Each mouse was positioned into the heating apparatus and monitored throughout the entire session. Heating times were varied from 5 to 20 minutes at 43 °C as measured by a thermocouple submerged in the water bath. Upon completion of heating, mice were removed from the apparatus and allowed to recover at ambient temperature for 6 hours. After the recovery period, 5 µM of DSG-Cy5.5 in saline was intravenously administered by tail vein injection and scanned in a Xenogen/Caliper IVIS-200 imaging system using the appropriate Cy5.5 filters with 0.15 seconds exposure time and medium binning. Mice were continuously anesthetized with 2% isoflurane and kept warmed during all image acquisitions.

Immunohistochemistry Procedure

Mice were killed using CO_2 gas and harvested mouse muscle samples were fixed in 10% buffered formalin solution and paraffin-embedded for immunohistochemistry using the same anti-HSP70 monoclonal antibody and counterstaining with hematoxylin. Immunohistochemistry procedure was performed by the pathology core service facility of the Methodist
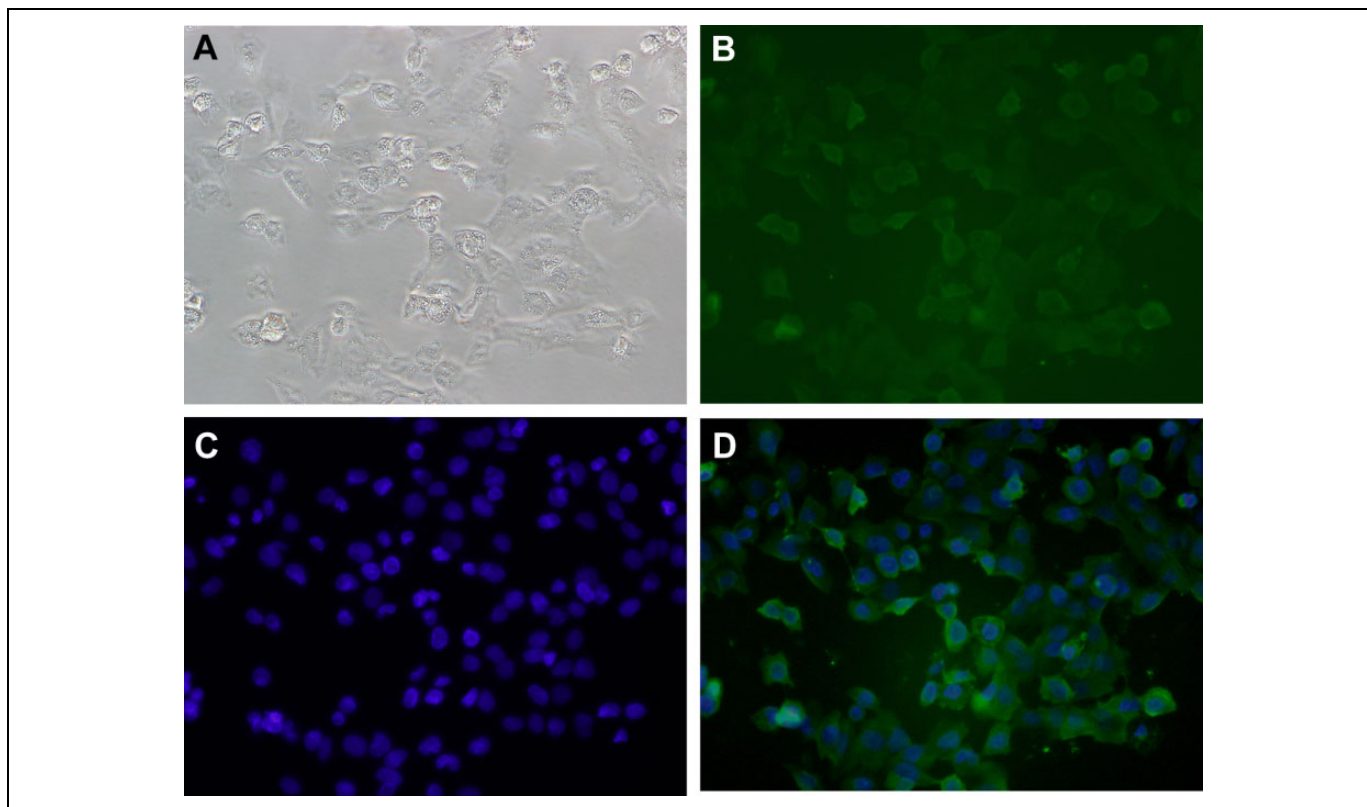
Figure 2. Immunohistochemistry of HSP70 induction by CuSO$_4$ in A549 cells. (A) Bright field phase contrast; (B) Anti-HSP70 staining; (C) DAPI counterstaining; (D) Overlay of anti-HSP and DAPI staining images. DAPI indicates 4′,6-diamidino-2-phenylindole; HSP70, heat shock protein 70.
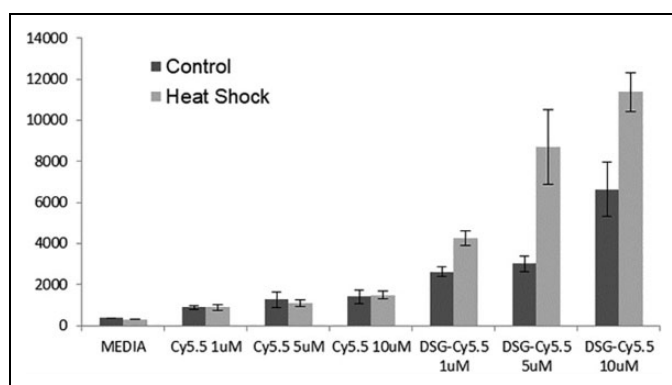

Figure 3. Human lung carcinoma (A549) cells were grown at 37 °C (dark gray) or heat shocked at 43 °C for 10 minutes in a tissue culture incubator (light gray) and allowed to recover for 6 hours. DSG-Cy5.5 was added to the culture media and allowed to incubate for 1 hour at 37 °C, followed by cell harvest and fluorescence measurements. Relative fluorescence values were plotted for the vehicle (media) and DSG-Cy5.5 at 3 final concentrations: 1, 5, and 10 μM. Error bars indicate standard error of the mean for 6 runs. Among the 3 concentrations of conjugates 5 μM and 10 μM were highly significant ($P < .001$) when compared with control and heat shock treatment. DSG indicates deoxyspergualin.

Hospital. All animal experiments were performed in strict compliance with a protocol approved by the institutional animal care and use committee of the Methodist Hospital Research Institute.

Results and Discussion

Deoxyspergualin was synthesized according to the published procedures with some modification of reaction conditions.[36-46] Briefly, the synthetic scheme for DSG-Cy5.5 is illustrated in Figure 1A-C. Orthogonally, protected spermidine derivative is one of the parts of DSG. Several methods leading to the synthesis of differentially protected spermidine have been described but it is not commercially available.[52-55] We have optimized the reaction conditions of this compound with high yield. Two protecting groups were used for the selective protection of 2 primary amino groups located at N^1 and N^8 and one secondary amino at N^4 in spermidine. Usually, the most popular amino protecting groups, that is, tert-butoxycarbonyl (Boc) and benzyloxycarbonyl (Z), meet the criteria to be used in the orthogonal protection of spermidine. The synthetic scheme for protected spermidine is illustrated in Figure 1A, the first step of the synthesis to obtained orthogonally protected N^4-tert-butoxycarbonyl-1,4-butanediamine **6** by the reaction of 1,4-butanediamine with di-tert-butyl dicarbonate in tetrahydrofuran in the presence of triethylamine at room temperature. Compound **6** was purified by column chromatography and isolated in 68% yield. Compound **7** was prepared by cyanoethylation reaction of the mono Boc-protected 1,4-butanediamine **6** and acrylonitrile in methanolic solution at −10 °C for 1 hour, warmed to room temperature, and continued for overnight stirring. Yield in this step was 74%. Secondary amino function in nitriles **7** was protected with
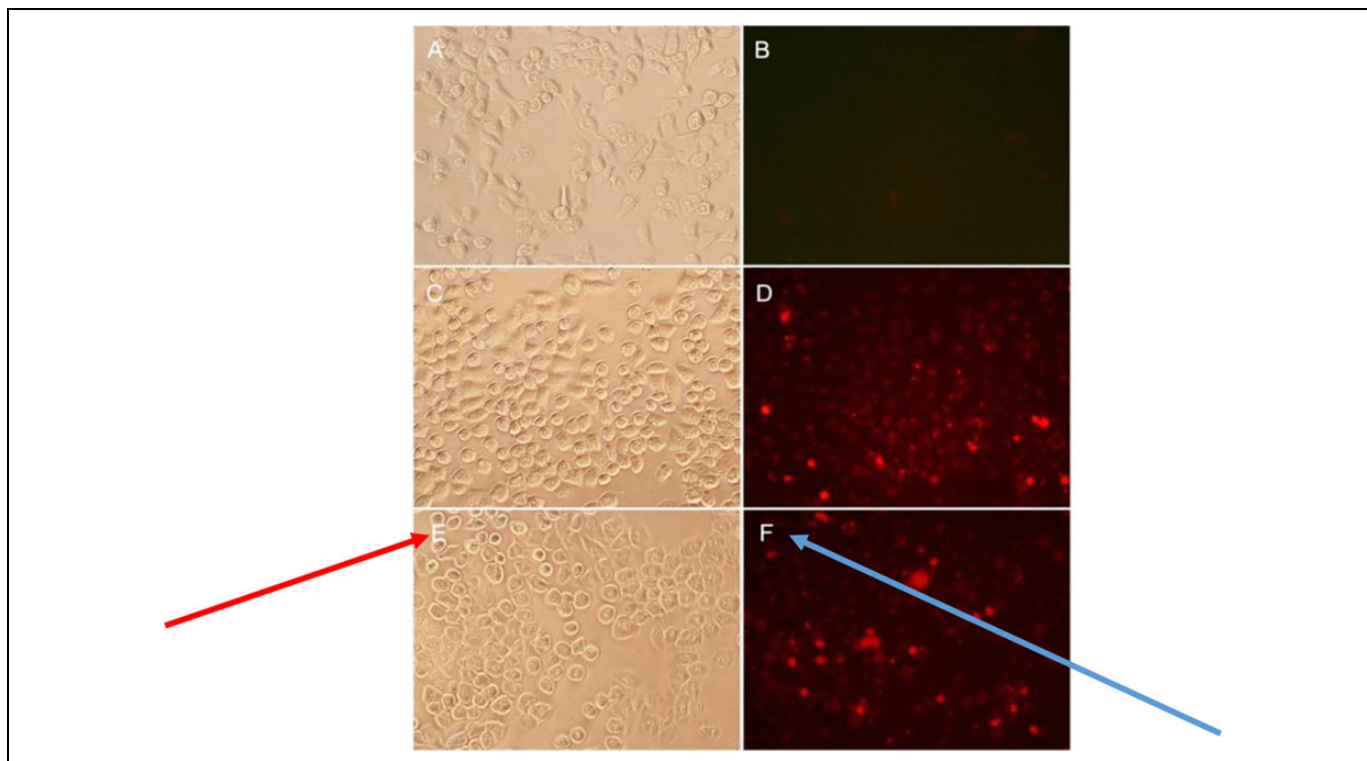
Figure 4. Detection of HSP70 by DSG-Cy5.5 in A549 cells. (A and B) Control at 37 °C, bright field and Cy5 filter, respectively; (C and D) Heat shock at 43 °C for 10 minutes, bright field, and Cy5.5 filter, respectively; (E and F) CuSO₄ induction, bright field, and Cy5.5 filter, respectively. DSG indicates deoxyspergualin; HSP70, heat shock protein 70.
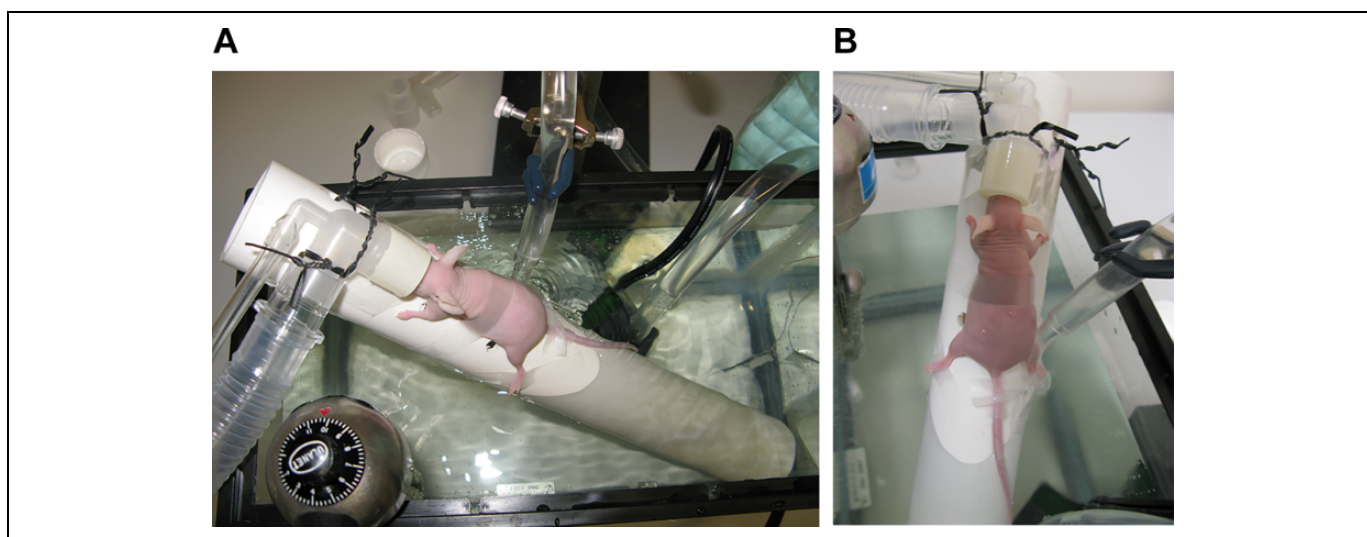

Figure 5. Small animal heating apparatus. (A) Top oblique view of mouse placed on platform with anesthesia nose cone (B) top view.

the use of benzyloxycarbonyl chloride protecting group in tetra-hydrofuran at room temperature to produced compound **8**. Purified yield in this step was 76%. The protected nitrile compound **8** was reduced with lithium aluminum hydride in dry ethyl ether solution at 0 °C to produced compound **9**, which was purified by silica gel column and isolated in 63% yield. The partially protected spermidine derivative **9** was subjected to acylation reaction with benzyloxycarbonyl chloride to obtained fully protected spermidine compound **10** in tetrahydrofuran at room temperature. Compound **10** was purified by column chromatography and isolated in 70% yield. Compound **11** was obtained by the reaction of compound **10** with trifluroacetic acid at 0 °C for 30 minutes and then warm up to room temperature for 3 hour, purified and isolated in 81% yield.
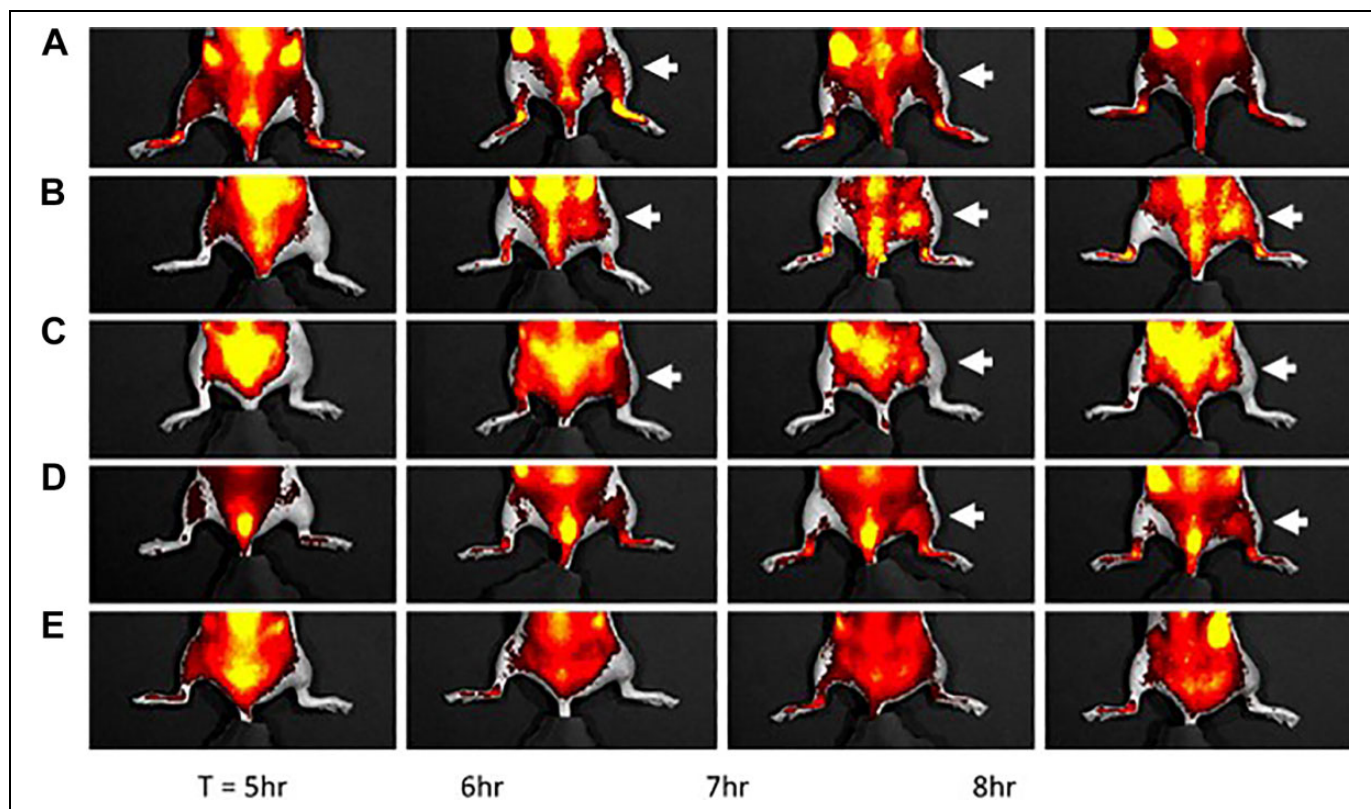
Figure 6. DSG-Cy5.5 fluorescence imaging of 5 mice treated in the right hind limb at 43 °C for: (A) 6 minutes, (B) 7 minutes, (C) 8 minutes, (D) 9 minutes, and (E) 10 minutes. DSG-Cy5.5 was administered at 5 hours post heating. Each mouse was imaged at 5 (immediately after injection of DSG-Cy5.5), followed at 6, 7, and 8 hours post heat treatment. Arrows indicate increased fluorescence signal in the treated limb. DSG indicates deoxyspergualin.

The synthetic scheme for DSG is illustrated in Figure 1B, compound **1** was prepared by reaction of 7-bromoheptanenitrile with concentrated hydrochloric acid at 40 °C. Compound **1** was purified by crystallization system and isolated in 81% yield. Nucleophilic substitution of the bromide with sodium azide in DMSO at 100 °C yielded **2** through microwave synthesis in which the azido function served as a protected primary amine need for elaboration of the guanidine function. The azido **2** was purified by column chromatography and isolated in 74% yield. Compound **3** was obtained by reaction of compound **2** with methyl 2-hydroxy-2-methoxyacetate in dichloromethane at 45 °C for overnight stirring. The formed methanol was trapped with molecular sieves.[56] Compound **3** was purified by flash chromatography and isolated in 70% yield. The resulting α-hydroxyglycine **3** was converted into a labile α-chloroglycine intermediate by treatment with thionyl chloride in dichloromethane at 50 °C. The chloro compound was as then treated with chiral benzylic alcohol [(S)-(-)-α-methyl-2-naphthalenemethanol] in presence of triethylamine to afford the diastereomers derivatives **4** in 75% total yield. Saponification of **4** gave the corresponding acid **5** yield in 96%, which was directly used to the next step. Compound **5** was coupled with the compound of **11**, N^1, N^4-bis (benzyloxycarbonyl) spermidine, using the DCC/ HOBT methodology in dichloromethane at room temperature to afford a mixture of the diastereomers compound **12** in 82% total yield.

Conversion of **12** to **13** was made in a 2-step one pot process. First the azido function was reduced without affecting the benzyloxy, and the benzyloxycarbonyl protective groups using $Ph_3P/H_2O/THF$[57] at 80 °C through microwaves synthesis for 4 hours. The primary amine was then reacted in situ with N, N′-bis(benzyloxycarbonyl)-S-methylisothiourea[58] to give a mixture of diastereomers derivatives **13**. The mixture of diastereomers was easily separated by simple flash chromatography to afford **13(a)** and **13(b)** in 41% and 37% yields, respectively. Final deprotection accomplished in one step using Pearlman's catalyst in 1(N) AcOH in methanol under 1 atm of hydrogen. It is worth mentioning that these experimental conditions provided triacetate **14** with high purity, hygroscopic solid without concomitant reductive dihydroxylation.[59] After that tris-acetate derivative is simply converted to its corresponding tris-hydrochloride derivative using 1N HCl at 0 °C, and followed by lyophilization. Compound **14** was purified by HPLC and isolated in 75% yield. This modification is thus extremely efficient for the synthesis of (+)-DSG with an overall yield of 18% to 22%.

The conjugate **15** (DSG-Cy5.5) was prepared by the reaction of **14** (DSG) with Cy5.5 mono NHS ester in 0.1 (M) sodium phosphate buffer (pH 8.2) at ambient temperature for
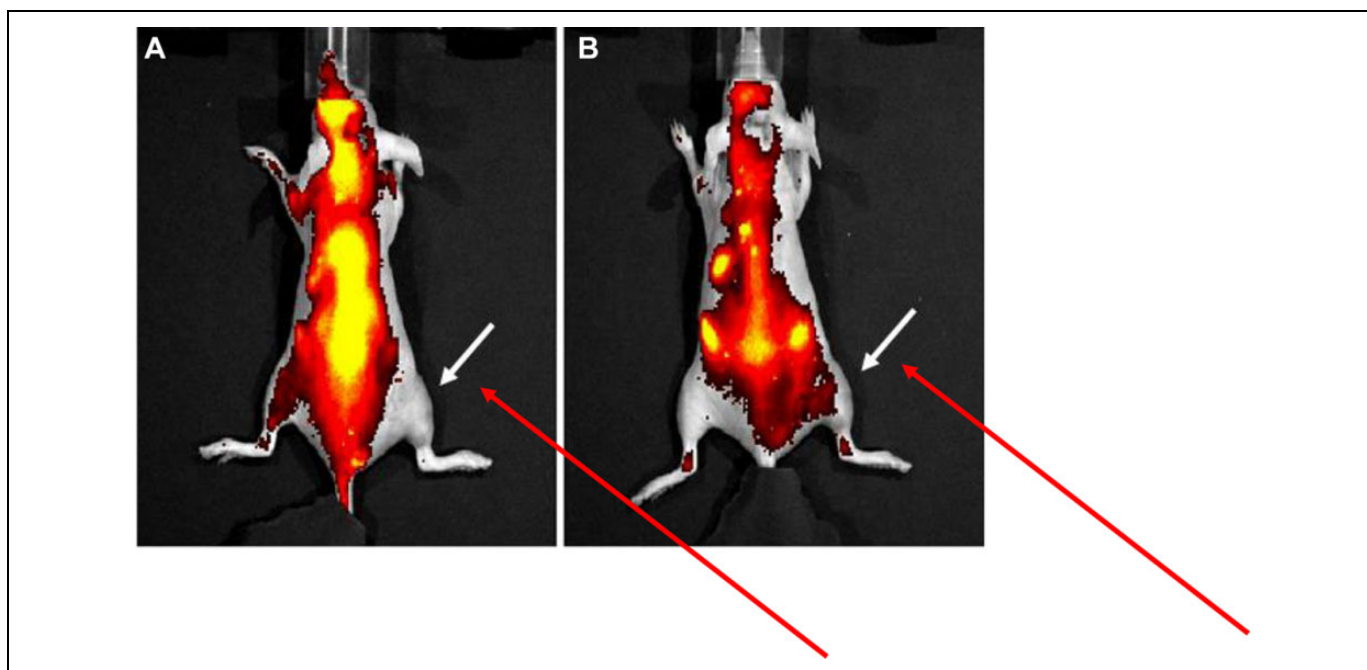
Figure 7. Detection of DSG-Cy5.5 at 24 hours. Mice were injected with a second dose of DSG-Cy5.5 and immediately imaged (A) followed by delayed imaging at one hour (B). Arrow points to the region in the right hind limb that continues to exhibit some fluorescence activity at 24 hours post heating. DSG indicates deoxyspergualin.

overnight and quenched by 5% acetic acid in water to make neutralization, Figure 1C. The crude product was purified by semi preparative HPLC and isolated in 60% yield. The pure conjugate **15** was stored in the dark at $-20\ ^\circ$C until use. The absorption and fluorescence emission characteristics of DSG-Cy5.5 conjugate was identical to the free Cy5.5, as apparent from the spectra measured in H_2O (data not shown). Samples were dissolved in PBS solution, pH 7.4 (PBS) and filter sterilized using a 0.2 micron mini-syringe filter (Whatman) prior to use. The HSP70 expression in human lung carcinoma cells (A549) was determined by immunohistochemical analysis which was inducted by $CuSO_4$ solution (Figure 2).

The deoxyspergualin conjugate (DSG-Cy5.5) was tested for cellular uptake in human lung carcinoma cells (A549) subjected to transient heat shock under aseptic conditions in a tissue culture incubator. As shown in Figure 3, cellular uptake of DSG-Cy5.5 is significantly increased following heat treatment at the concentration tested. A 5 μM and 10 μM concentrations were highly significant ($P < .001$) when compared with control and heat shock treatment. Cy5.5 alone was used as control at the same molar concentrations showed no significant cellular uptake. Figure 4 also shown that the cellular uptake of DSG-Cy5.5 is significantly increased following heat treatment at the 5 μM concentration in lung carcinoma (A549) cell line.

This in vitro result prompted us to evaluate the in vivo uptake of this compound by testing for accumulation in normal tissue subjected to localized hyperthermia. Results from a study testing 43 $^\circ$C for 6 to 10 minutes are shown in Figure 6A-E. Image processing was performed on the Living

Image v3.0 software without background subtraction or autofluorescence correction. As evident from the fluorescence images, there is increased signal intensity in the right hind limb indicated by arrows. Prominent signal intensity is noted at approximately 7 minutes at 43 $^\circ$C and imaged at 7 to 8 hours post-heat treatment. The majority of the nonspecific thoracic and abdominal fluorescence signal is largely due to autofluorescence (and likely from high-chlorophyll content diet) as determined by imaging of uninjected animals (data not shown). After approximately 24 hours, a second intravenous dose was administered and imaged immediately and at 1 hour postinjection resulting in detectable signal in the treated limb (Figure 7). This result corroborates the persistent HSP70 staining observed in the tissue culture experiment (Figure 4D). Following completion of imaging studies, mice were killed and soft tissue from the hind limbs were harvested and fixed in 10% formalin, sectioned, and immunostained with anti-HSP70 antibody. Localized disruption of the skeletal muscle fibers was observed with heat treatment at 43 $^\circ$C for 10 minutes, suggesting thermal injury (Figure 8). Tissue harvested at the time of killing 6 hours post heating were fixed and stained for HSP70 protein. Robust immunohistochemical staining for HSP70 was observed in the heated tissue (Figure 8B) and not in the untreated control (Figure 8A). This observation provides supporting evidence for the postulated localization mechanism of DSG-Cy5.5 to the site of heat shock. Nonetheless, the experimental results present in this work support the hypothesis that accumulation of a composite small molecule may be controlled "on demand" by the induction of endogenous intracellular targets.
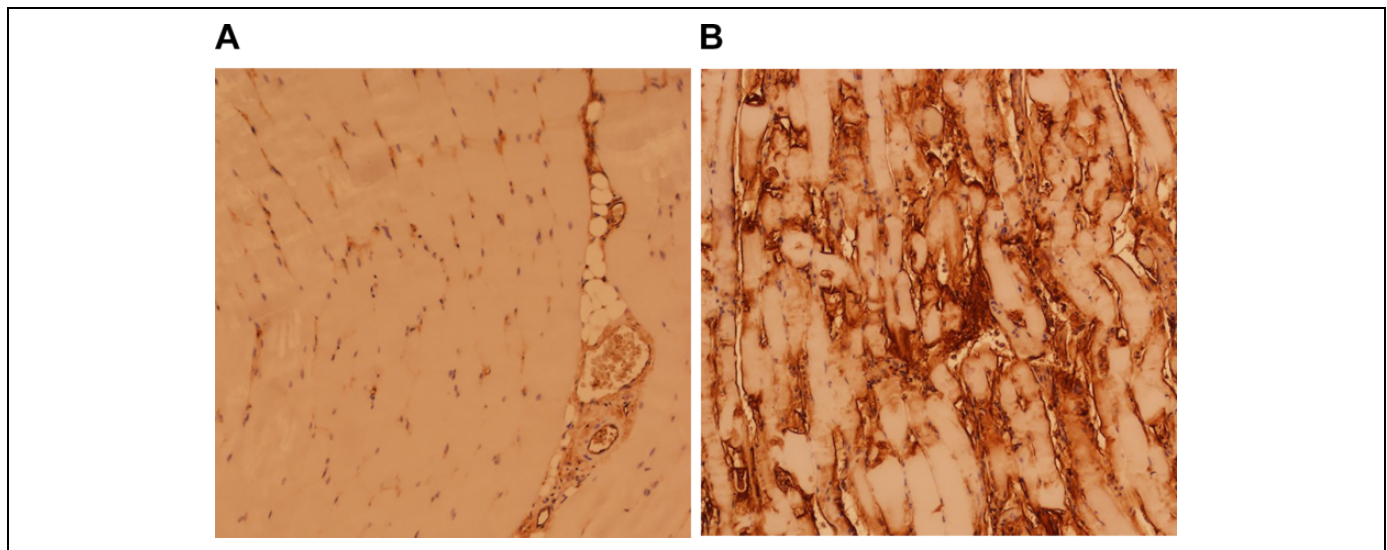
Figure 8. Immunostaining for HSP70 in soft tissue harvested 6 hours post heating at 43 °C for 10 minutes. (A) Unheated contralateral limb; (B) Heated limb. HSP70 indicates heat shock protein 70.

In this study, DSG-Cy5.5 was significantly accumulated both in tissue culture and in experimental mice with comparable findings. Further translational evaluation of DSG-Cy5.5 is warranted.

Conclusion

This study demonstrates proof of concept for the novel approach of imaging an inducible target using an endogenous protein involved in stress response. According to our findings, DSG-Cy5.5 may serve as a valuable optical probe for imaging and also to investigate the role of HSP in cancer biology in future.

Declaration of Conflicting Interests

The author(s) declared no potential conflicts of interest with respect to the research, authorship, and/or publication of this article.

ORCID iD

Pradip Ghosh, Ph.D. https://orcid.org/0000-0003-0666-8602

References

1. Schmitt E, Gehrmann M, Brunet M, Multhoff G, Garrido C. Intracellular and extracellular functions of heat shock proteins: repercussions in cancer therapy. *J Leukoc Biol*. 2007;81(1):15–27.

2. Soti C, Nagy E, Giricz Z, Vigh L, Csermely P, Ferdinandy P. Heat shock proteins as emerging therapeutic targets. *Br J Pharmacol*. 2005;146(1):769–780.

3. Calderwood SK, Theriault JR, Gong J. Message in a bottle: role of the 70-kDa heat shock protein family in anti-tumor immunity. *Eur J Immunol*. 2005;35(9):2518–2527.

4. Garrido C, Brunet M, Didelot C, Zermati Y, Schmitt E, Kroemer G. Heat shock proteins 27 and 70: antiapoptotic proteins with tumorigenic properties. *Cell Cycle*. 2006;5(22):2592–2601.

5. Ciocca DR, Calderwood SK. Heat shock proteins in cancer: diagnostic, prognostic, predictive, and treatment implications. *Cell Stress Chaperones*. 2005;10(2):86–103.

6. Kregel KC. Heat shock proteins: modifying factors in physiological stress responses and acquired thermotolerance. *J Appl Physiol (1985)*. 2002;92(5):2177–2186.

7. Macario AJ, De Macario EC. Molecular chaperones: multiple functions, pathologies, and potential applications. *Front Biosci*. 2007;12:2588–2600.

8. Murphy ME. The HSP70 family and cancer. *Carcinogenesis*. 2013;34(6):1181–1188.

9. Wang X, Meijuan C, Jing Z, Xu Z. HSP27, 70 and 90, anti-apoptotic proteins, in clinical cancer therapy (review). *Int J Oncol*. 2014;45(1):18–30.

10. Lee AS. GRP78 induction in cancer: therapeutic and prognostic implications. *Cancer Res*. 2007;67(8):3496–3499.

11. Liu T, Christopher KD, Shousong C. Comprehensive review on the HSC70 functions, interactions with related molecules and involvement in clinical diseases and therapeutic potential. *Pharmacol Ther*. 2012;136(3):354–374.

12. Rérole AL, Gaëtan J, Carmen G. Hsp70: anti-apoptotic and tumorigenic protein. *Methods Mol Biol*. 2011;787:205–230.

13. Jäättelä M, Wissing D, Bauer PA, Li GC. Major heat shock protein hsp70 protects tumor cells from tumor necrosis factor cytotoxicity. *EMBO J*. 1992;11(10):3507–3512.

14. Kubota H, Soh Y, Eri I, et al. Increased expression of co-chaperone HOP with HSP90 and HSC70 and complex formation in human colonic carcinoma. *Cell Stress Chaperones*. 2010; 15(6):1003–1111.

15. Moghanibashi M, Ferdous RJ, Zahra-Soheila S, et al. Esophageal cancer alters the expression of nuclear pore complex binding protein Hsc70 and eIF5A-1. *Funct Integr Genomics*. 2013; 13(2):253–260.

16. Bakkenist CJ, Koreth J, Williams CS, Hunt NC, McGee JO. Heat shock cognate 70 mutations in sporadic breast carcinoma. *Cancer Res*. 1999;59(17):4219–4221.

17. Rusin M., Helena Z, Małgorzata K, et al. Intronic polymorphism (1541-1542delGT) of the constitutive heat shock protein 70 gene has functional significance and shows evidence of association with lung cancer risk. *Mol Carcinog*. 2004;39(3):155–163.

18. Sandoval JA, Derek JH, Heather AW, et al. Novel peptides secreted from human neuroblastoma: useful clinical tools? *J Pediatr Surg*. 2006;41(1):245–251.

19. Rohde M, Daugaard M, Jensen MH, Helin K, Nylandsted J, Jaattela M. Members of the heat-shock protein 70 family promote cancer cell growth by distinct mechanisms. *Genes Dev*. 2005; 19(5):570–582.

20. Seo JS, Park YM, Kim JI, et al. T cell lymphoma in transgenic mice expressing the human Hsp70 gene. *Biochem Biophys Res Commun*. 1996;218(2):582–587.

21. Sliutz G, Karlseder J, Tempfer C, Orel L, Holzer G, Simon MM. Drug resistance against gemcitabine and topotecan mediated by constitutive hsp70 overexpression in vitro: implication of quercetin as sensitiser in chemotherapy. *Br J Cancer*. 1996;74(2):172–177.

22. Mosser DD, Morimoto RI. Molecular chaperones and the stress of oncogenesis. *Oncogene*. 2004;23(16):2907–2918.

23. Whitesell L, Lindquist S. Inhibiting the transcription factor HSF1 as an anticancer strategy. *Expert Opin Ther Targets*. 2009;13(4): 469–478.

24. Powers MV, Workman P. Inhibitors of the heat shock response: biology and pharmacology. *FEBS Lett*. 2007;581(19):3758–3769.

25. Nishikawa K, Shibasaki C, Hiratsuka M, Arakawa M, Takahashi K, Takeuchi T. Antitumor spectrum of deoxyspergualin and its lack of cross-resistance to other antitumor agents. *J Antibiot*. 1991;44(10):1101–1109.

26. Plowman J, Harrison SD Jr, Trader MW, et al. Preclinical anti-tumor activity and pharmacological properties of deoxyspergualin. *Cancer Res*. 1987;47(3):685–689.

27. Nemoto K, Abe F, Takita T, Nakamura T, Takeuchi T, Umezawa H. Suppression of experimental allergic encephalomyelitis in guinea pigs by spergualin and 15-deoxyspergualin. *J Antibiot (Tokyo)*. 1987;40(8):1193–1194.

28. Nemoto K, Ito J, Abe F, Nakamura T, Takeuchi T, Umezawa H. Suppression of humoral immunity in dogs by 15-deoxyspergualin. *J Antibiot (Tokyo)*. 1987;40(7):1065–2056.

29. Nemoto K, Ito J, Hayashi M, et al. Effects of spergualin and 15-deoxyspergualin on the development of graft-versus-host disease in mice. *Transplant Proc*. 1987;19(4):3520–3521.

30. Masuda T, Mizutani S, Iijima M, et al. Immunosuppressive activity of 15-deoxyspergualin and its effect on skin allografts in rats. *J Antibiot (Tokyo)*. 1987;40(11):1612–1618.

31. Nadeau K, Nadler SG, Saulnier M, Tepper MA, Walsh CT. Quantitation of the interaction of the immunosuppressant deoxyspergualin and analogs with Hsc70 and Hsp90. *Biochemistry*. 1994; 33(9):2561–2567.

32. Nadler SG, Tepper MA, Schacter B, Mazzucco CE. Interaction of the immunosuppressant deoxyspergualin with a member of the Hsp70 family of heat shock proteins. *Science*. 1992;258(5081): 484–486.

33. Hiratsuka M, Hiroshi K, Katsutoshi T, Tomio T, Mitsuo M. Cytostatic effect of deoxyspergualin on a murine leukemia cell line L1210. *J Cancer Res*. 1991;82(10):1065–1068.

34. Nishikawa K, Shibasaki C, Uchida T, Takahashi K, Takeuchi T. The nature of in vivo cell-killing of deoxyspergualin, and its implication in combination with other antitumor agents. *J Antibiot (Tokyo)*. 1991;44(11):1237–1246.

35. Oikawa T, Hasegawa M, Morita I, et al. Effect of 15-deoxyspergualin, a microbial angiogenesis inhibitor, on the biological activities of bovine vascular endothelial cells. *Anticancer Drugs*. 1992;3(3):293–299.

36. Durand P, Peralba P, Renaut P. A new efficient synthesis of the immunosuppressive agent (+/-)-15-deoxyspergualin. *Tetrahedron*. 2001;57(14):2757–2760.

37. Lebreton L, Jost E, Carboni B, et al. Structure-immunosuppressive activity relationships of new analogues of 15-deoxyspergualin. 2. structural modifications of the spermidine moiety. *J Med Chem*. 1999;42(23):4749–4763.

38. Raymond JB, James SM. Total synthesis of (&)-15-deoxyspergualin. *J Org Chem*. 1987;52(9):1700–1703.

39. Philippe D, Philippe R, Patrice R. 15-Deoxyspergualin: a new and efficient enantioselective synthesis which allows the definitive assignment of the absolute configuration. *J Org Chem*. 1998; 63(26):9723–9727.

40. Takeuchi T, Iinuma H, Kunimoto S, et al. A new antitumor antibiotic, spergualin: isolation and antitumor activity. *J Antibiot (Tokyo)*. 1981;34(12):1619–1621.

41. Umezawa H, Kondo S, Iinuma H, et al. Structure of an antitumor antibiotic, spergualin. *J Antibiot (Tokyo)*. 1981;34(12): 1622–1624.

42. Kondo S, Iwasawa H, Ikeda D, et al. The total synthesis of spergualin, an antitumor antibiotic. *J Antibiot (Tokyo)*. 1981;34(12): 1625–1627.

43. Umeda Y, Moriguchi M, Kuroda H, et al. Synthesis and antitumor activity of spergualin analogues. I. chemical modification of 7-guanidino-3-hydroxyacyl moiety. *J Antibiot (Tokyo)*. 1985;38(7): 886–898.

44. Umeda Y, Moriguchi M, Ikai K, et al. Synthesis and antitumor activity of spergualin analogues. III. novel method for synthesis of optically active 15-deoxyspergualin and 15-deoxy-11-Omethyl-spergualin. *J Antibiot (Tokyo)*. 1987;40(9):1316–1324.

45. Lebreton L, Annat J, Derrepas P, Dutartre P, Renaut P. Structure-immunosuppressive activity relationships of new analogues of 15-deoxyspergualin. 1. structural modifications of the hydroxyglycine moiety. *J Med Chem*. 1999;42(2):277–290.

46. Nishizawa R, Takei Y, Yoshida M, et al. Synthesis and biological activity of spergualin analogues. I. *J Antibiot (Tokyo)*. 1988; 41(11):1629–1643.

47. Ghosh P, Li KCP, Lee D. Radiosynthesis of [¹⁸F]-Fluoromethyl deoxyspergualin for molecular imaging of heat shock proteins. *Appl Radiat Isot*. 2011;69(3):609–613.

48. Wang X, Zhang J, Wu H, Li Y, Conti SP, Chen K. PET imaging of Hsp90 expression in pancreatic cancer using a new ⁶⁴Cu-labeled dimeric Sansalvamide A decapeptide. *Amino Acids*. 2018;50(7): 897–907.

49. Niu G, Li Z, Cao Q, Chen X. Monitoring therapeutic response of human ovarian cancer to 17-DMAG by noninvasive PET imaging with ⁶⁴Cu-DOTA-trastuzumab. *Eur J Nucl Med Mol Imaging*. 2009;36(9):1510–1519.

50. Gehrmann M, Stangl S, Foulds AG, et al. Tumor imaging and targeting potential of an Hsp70 derived 14-mer peptide. *PLoS One*. 2014;9(8):e105344.

51. Neuhaus-Steinmetz U, Rensing L. Heat shock protein induction by certain chemical stressors is correlated with their cytotoxicity, lipophilicity and protein-denaturing capacity. *Toxicology*. 1997; 123(3):185–195.

52. Araujo MJSMP, Ragnarsson U, Amaral Trigo MJSA, Almeida MLS. Synthesis of carbamate protected spermidine homologues through alkane-α, ω-diamines. *J Chem Res*. 1996;2(3): 2143–2161.

53. Blagbrough IS, Moya E. Total synthesis of polyamine spider toxin argiotoxin-636 by a practical reductive alkylation strategy. *Tetrahedron Lett*. 1995;36(15):9393–9396.

54. Edwards ML, Stemerick DM, Bitonti AJ, et al. Antimalarial polyamine analogs. *J Med Chem*. 1991;34(2):569–574.

55. Bradley JC, Vigneron JP, Lehn JM. A rapid and efficient preparation of linear and macrocyclic polyamine bolaphiles. *Synth Commun*. 1997;27(1):2833–2845.

56. Daumas M, Vo Quang L, Le Goffic F. An improved synthesis of Methyl 2-N-formylamino-2-(dimethoxyphosphinyl)-acetate. *Synth Commun* 1990;20(3):3395–3401.

57. Knouzi N, Vaultier M, Carrie R. Reduction of azides by triphenylphosphine in the presence of water: a general and chemoselective access to primary amines. *Bull Soc Chim Fr*. 1985;5(1):815–819.

58. Tian Z, Edward P, Roeske RW. Synthesis of optically pure C alpha-methyl-arginine. *Int J Pept Protein Res*. 1992;40(2):119–126.

59. Auerbach J, Zamore MCF, Weinreb SM. N-Methylation of amides, lactams, and ureas. *J Org Chem*. 1976;41(4):725–726.